GENERAL GROUP VI TRANSITION NANOSTRUCTURED METAL OXIDES AND THEIR INCLUSION INTO SOLID MATRICES BY A SOLUTION-SOLID APPROACH

C. DÍAZ [1], M.L. VALENZUELA [2*], LILIA ZEPEDA [1], PABLO HERRERA [1] AND CONSTANZA VALENZUELA [1]*

[1]*Departamento de Química, Facultad de Química, Universidad de Chile, La Palmeras 3425, Nuñoa, casilla 653, Santiago de Chile, Chile.*
[2]*Instituto de Ciencias Químicas Aplicadas, Grupo de Investigación en Energía y Procesos Sustentables, Facultad de Ingeniería, Universidad Autónoma de Chile, Av. El Llano Subercaseaux 2801, San Miguel, Santiago de Chile, Chile.*

ABSTRACT

A facile and general solution//solid-state (SSS) approach to the synthesis of nanostructured metal oxides Cr_2O_3, MoO_3 and WO_3 was investigated. They are made from solid-state pyrolysis of the metal- macromolecular precursors PS-co-4-PVP●MCl_n and Chitosan●MCl_n with M= Cr, Mo and W, which were easily prepared by direct reaction of the salts $CrCl_3$, $MoCl_4$ and WCl_4 with the respective polymer. The size and morphology of the products, the nanostructured oxides Cr_2O_3, MoO_3 and WO_3 depend on the polymer and on the coordination degree of the precursor**.** Cr_2O_3 as well as WO_3, prepared from this method were included in silica and Titania matrix using an also solution//solid-state approximation. The nanoparticles of Cr_2O_3 and WO_3 are in general distributed with uniformity within the amorphous silica. A probable formation mechanism of the Cr_2O_3, MoO_3 and WO_3 nanoparticles was proposed. The nanocomposites Cr_2O_3//SiO_2 and WO_3//SiO_2 could be useful materials in catalysis.

Keywords: Solid-state, pyrolysis, nanostructured, metal oxide

INTRODUCTION

Among the metal-ligand coordination compounds, the macromolecular complexes [1] can be considered as a special case, where the ligand has multiple coordination sites. The preparation of such metal multi-sites ligands is usually difficult because of metal ions must coordinate hundreds and sometimes thousands of coordination sites. This process is often of a slow kinetics, being the products usually insoluble and of poor characterization. Thus, these macromolecular complexes rarely reach the 100%-degree coordination [2-5]. In spite of this, this particular type of multi-coordination compounds have attracted much the attention due to their interesting applications in the materials science. For instance the metallic derivate from polyphosphazenes affords, after pyrolysis at 800 °C under air, nanostructured materials of the type M° and M_xO_y//$M_x(PO_Y)_z$ [6-9] .The metallic phosphate phases normally appears due to the presence of phosphorus atoms in the polymeric chain.

Metal oxides have attracted great interest for their applications as anode materials for lithium batteries [10,11], catalysis [12,13], sensors [14], solar cells [15], solid-state transistors [16] and metal ion removal [17]. Although several solution methods to prepare metal oxides have been reported [18-22] few solid-state routes have appeared [23,24]. The aim of developing solid-state methods to prepare nanoparticles stems mainly from their possible application in solid-state materials and powder-oriented applications, from thin film metal deposition to noble metal nanoparticle-carbon catalysts, oxide growth, photonic and dielectric materials, to new materials for Li-ion rechargeable batteries. The ability to rationally prepare metallic and metal oxide nanoparticles stems from the exploring methods for alternative nanoscale metal deposition in solid-state nanoelectronics and nanotechnology [25-28] and the benefit of being able to deposit both metals and dielectric or semiconducting oxides, both from the same base route. Issues including limitations on good mechanical and thermal stability of nanoscale metal have been found related to certain deposition methods for these metals. Most of this application requires pure phase metal oxides.

For group VI metal oxide there not a general method to prepare these nanostructured materials. For instance, using $W(CO)_6$ as precursors the $W_{18}O_{49}$ nanostructured molibdenum oxide was obtained [29]. On the other hand the Cr_2O_3 nanostructured nanoparticles was obtained from the thermal treatment of the carbene Fischer $(CO)_5CrC(Ph)(OMe)$ [30].The nanostructured MoO_3 was obtained from a hydrothermal method using $(NH_4)_6Mo_7O_{24}$●$4H_2O$ as source of Mo [31]. Alternatively other methods have also been used to obtain the nanostructured Cr_2O_3, MoO_3 and WO_3 [32-38]. On the other hand, the thermal treatment $\{[NP(O_2C_{12}H_8)]_{0.8}[NP(OC_6H_4CH_2CN$●$[Cr(CO)_5]_{0.13})_2]_{0.18}\}_n$ results in the formation of nanometer-size metal oxide particles [38].

We have developed a new solid-state method to prepare phase pure metal oxide nanoparticles from the macromolecular complexes Chitosan●MXn and PS-co-4-PVP●MXn (PS-co-4-PVP = Poly(styrene-co-4-vinylpyridine)) see scheme 1. In this paper the phase pure Cr_2O_3, MoO_3 and WO_3 were prepared using this synthetic approach. We have chosen Chitosan because of it is a cheap commercial product and by their effective coordinative properties to ion metal. Chitosan [39-41] is a polysaccharide obtained by deacetylation of natural chitin, which is one of the important natural polymers constituting the shells of crustaceans and the cell wall of many fungi. Due to its available from the NH_2 groups and the OH moieties present in the polysaccharide chains; it can bind metal ions -in solution- forming macromolecular metal complexes [42-44]. Although the ability to retain metal ions in solution, Chitosan has been widely studied and previously reported, solid-state-macromolecular complexes have been not well characterized. Particularly for several some Cu /Chitosan complexes, some X-ray and ESR studies have been performed [45-47]. Chitosan can act as solution template/stabilizer for the formation of nanoparticles [47-55]. Some biological applications [54-55] including biosensors for glucose have been reported [58]. In addition, Chitosan as support for catalysis processes have been also described [56].

On the other hand, Poly(styrene-co-4vinylpyridine) is useful functional copolymer due to the vinylpyridine block which binds metal ions and the styrene groups to facilitate stable macromolecular complexes 1, [53-56]. It has also been used to aid in selective facet growth in noble metal nanoparticle. PS-*b*-4-PVP has been used in solution as a template/stabilizer of metals and other nanoparticles [57-60].

Although several solution methods to prepare nanostructured Cr_2O_3, MoO_3 and WO_3 oxides few solid-state routes have been informed [61-67]. Using a solid state approach with precursors having the organometallic fragment $W(CO)_5$ linked to oligo and poly-phosphazene mixtures of $W/WO_3/WP_2O_3$ mixtures are obtained [68] while that using the organometallic derivatives of poly(styrene-co-4vinylpyridine), $[CH_2CH(C_6H_5)]_{0.1}[CH_2CH(C_5H_4N$●$ML_n)]_{0.9}\}_n$; ML_n = $W(CO)_5$,as precursors pure WO_3 obtained [69] . On the other hand from the $N_3P_3[OC_6H_4CH_2CN{\cdot}Mo(CO)_5]_6$ (**I**) and $N_3P_3[OC_6H_4CH_2CN{\cdot}Mo(CO)_5]_6$ (**II**) precursors pure phase MoO_3 was obtained [69].

**Corresponding author email: maria.valenzuela@uautonoma.cl*

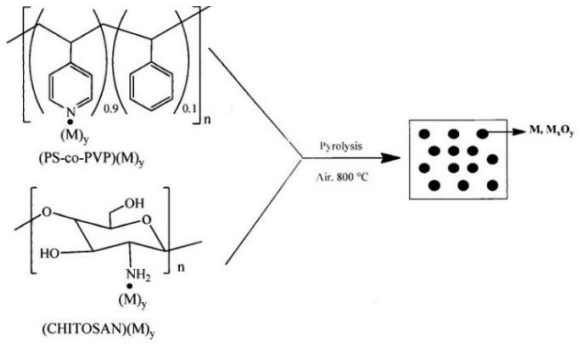

Figure 1. Schematic representation of the PS-co-4-PVP●MXn and Chitosan●MXn precursors.

The scheme shows the M-N(pyridine) and M-NH_2 coordination site but not the structure of the metal-polymer complexes. Here M represent the respective metallic salt linked to the polymeric chain i.e. $CrCl_3$, $MoCl_4$ and WCl_4.

Here we present a general and reliable solid-state method for to obtain the respective metal oxide nanoparticles Cr_2O_3, MoO_3 and WO_3 from the PS-co-4-PVP●MXn and Chitosan●MXn precursors and also useful for their inclusion into solid matrix SiO_2.

EXPERIMENTAL

Materials and Common Procedures

$CrCl_3 \cdot 2H_2O$, $MoCl_4$ and WCl_4, from Aldrich were used as received. Chitosan (Aldrich) of low molecular weight was used as receive. An estimation of the molecular weight was performed by viscosimetry. The average molecular weight was determined from the Mark-Houwink equation and values of [h] obtained using parameter previously reported by Rinaudo et al [47]. The solvent used was a aqueous solution of acetic acid, NaCl and urea. The value was Mw = 61.000. All the reactions were performed in CH_2Cl_2 as solvent. Poly(styrene-co-4vinylpyridine) Aldrich with a 90 % of pyridine groups was used as received.

General Procedure

Metal-macromolecular complexes (1), (2) and (3) were prepared according to published procedures [69-71]. In a typical synthesis, the respective metallic salt was added in a Schlenk tube over a CH_2Cl_2 solvent under magnetic stirring and then the respective polymer PSP-co-4-PVP or Chitosan was added amount according to a 1:1, molar ratio. Reaction time and other details for each metallic salts reaction are given in Table 1 of Supplementary Materials. After this, the supernatant solution (if the solid decanted) was extracted with a syringe and the solid was dried under reduced pressure. Experimental details for the reactions are given in table see Table 1 of Supplementary data S1. The precursor PS-co-4-PVP●$CrCl_3$//SiO_2 and Chitosan●$CrCl_3$//SiO_2 and PS-co-4-PVP●WCl_4//SiO_2, Chitosan●WCl_4//SiO_2 were prepared incorporating to the reaction, TEOS for generating SiO_2 [71] .Experimental details are given in Table 1 of Supplementary Materials.

Characterization of the precursors

Owing their insolubility characterization of the precursors was made only by, IR spectroscopy.

Pyrolysis of the precursors

The pyrolysis experiments were made by pouring a weighed portion (0.05–0.15 g) of the metal-polymer precursor 1-6 into aluminum oxide boats that were placed in a furnace (Daihan oven model Wise Therm FHP-12) under a flow of air, heating from 25°C to upper temperature limits of 300°C, and then to 800 °C, followed by annealing for 2-4 h in each case. The heating rate was consistently maintained at 10 °C min^{-1} for all experiments. Solid pyrolytic samples were characterized by X-Ray diffraction of powders (XRD) scanning electron microscopy (SEM), high resolution transmission electron microscopy (HRTEM), Fourier transform infra-red (FTIR) spectroscopy, and thermogravimetric (TG) and differential scanning calorimetric (DSC) analysis. SEM images were acquired with a Philips EM 300 scanning electron microscope. Energy dispersive X-ray analysis (EDAX) was performed on a NORAN Instrument micro-probe attached to a JEOL 5410 scanning electron microscope. Transmission electron microscopy (TEM) experiments were performed using a FEI Tecnai T20 microscope, operated at 200 kV, in order to analyses the average size, distribution and morphology of the particles. High-resolution transmission electron microscopy (HRTEM) was performed using a JEOL 2000FX microscope at 200 kV. Interplanar distances were measured using the Gatan Digital Micrograph software. The TEM samples were prepared by dispersing pyrolized material onto copper grids, previously sonicated under ethanol media and then dried at room temperature. For high-resolution examination of graphitic carbons, flakes of sonicated carbons were dispersed on grids and examined under SEM to determine their thickness. X-ray diffraction (XRD) was conducted at room temperature on a Siemens D-5000 diffractometer with θ-2θ geometry. The XRD data was collected using Cu-Kα radiation (40 kV, 30 mA). FTIR measurements were performed on a Perkin Elmer FTIR spectrophotometer model Spectrum BXII.

RESULTS AND DISCUSSION

Macromolecular complexes

The direct reaction of the metallic salts $CrCl_3$, $MoCl_4$ and WCl_3 with the respective polymer Chitosan or PSP-co-4-PVP in CH_2Cl_2 as solvent affords very stable insoluble solids with colors stem from the coordination of the metal ion to the polymer. For instance precursors, green from the (Chitosan)$(CrCl_3)_x$ and PS-co-4-PVP●$(CrCl_3)_x$ see S_1 Supplementary data.

Coordination of the metal ions to the coordinating groups of both polymers was achieved by IR spectroscopy. For Chitosan-metal complexes the coordination was evident from the broad ν(OH) in Chitosan [44,46,70] which becomes unfolded upon coordination, appearing a new band around 3100 cm^{-1}. On the other hand for poly(styrene-co-4-vinylpyridine) the coordination was confirmed by the emergence of a new band centered at 1600 cm^{-1} characteristic of pyridine coordination [69,70]. Selected data for the precursor PS-co-4-PVP●$(MoCl_4)_n$ and Chitosan●$(MoCl_4)_n$ are shows in Supplementary data, S2.

Pyrolysis of Macromolecular complexes

The pyrolytic products were characterized by XRD powers. Illustrative XDR the pyrolytic products Cr_2O_3, MoO_3 and WO_3 from the respective precursors PS-co-4-PVP●MXn are shown in supplementary data S3, figure A. For precursors **(2)** sharp peaks –among other less intense-were obtained at corresponding to the planes (012), (104), (110), (113), (024) and (116) indicate the rhombohedra Cr_2O_3 [32]. Fig. B of S3 shows the XRD peaks which can be indexed to orthorhombic crystal MoO_3 (JCPDS card N° 00-005-0508). Main peak was observed at (020), (110), (040) (021) (111), (112), (060), see Fig S3. Thus the crystal phase is somewhat different to that obtained from precursors $N_3P_3[OC_6H_4CH_2CN{\cdot}Mo(CO)_5]_6$ (**I**) and $N_3P_3[OC_6H_4CH_2CN{\cdot}Mo(CO)_5]_6$ (**II**) precursors [69] were some fraction of lamellar was also observed. The observed XRD pattern is similar to that of MoO_3 obtained by another solution method. [33].

Figure C of S3 shows the XRD peaks which can be indexed to monoclinic crystal WO_3 (JCPDS card N^{ro} 01-083-0950). Main peak was observed at (002), (020), (200) (120) (-120), (112), (022), (220) (-202) and (400) see Fig S3. The observed XRD pattern is similar to that of pyrolytic residue from the organometallic precursors $[CH_2CH(C_6H_5)]_{0.1}[CH_2CH(C_5H_4N{\bullet}(W(CO)_5)]_{0.9}\}_n$ [68].

As is usually observed for nanoparticles produced by thermal methods the size and shapes exhibits wide distributions being usually rather big sizes and with a variety of shapes [23]. TEM images for the Cr precursors show a clear dependence of the size with the molar ratio as shown in figure 2. There is no clear explanation for this finding, although it could be related with the form of how the metallic centers are distributed along the polymeric chain. HRTEM images show different morphologies for the pyrolytic products from the chromium oxide. Figure 2 (f) confirmed the formation of Cr_2O_3, as the interplanar distance of 0.25 nm (110) was measured. EDS analysis see figure 2d shows as expected the presence of Cr and O (also Cu arising from the copper grid).

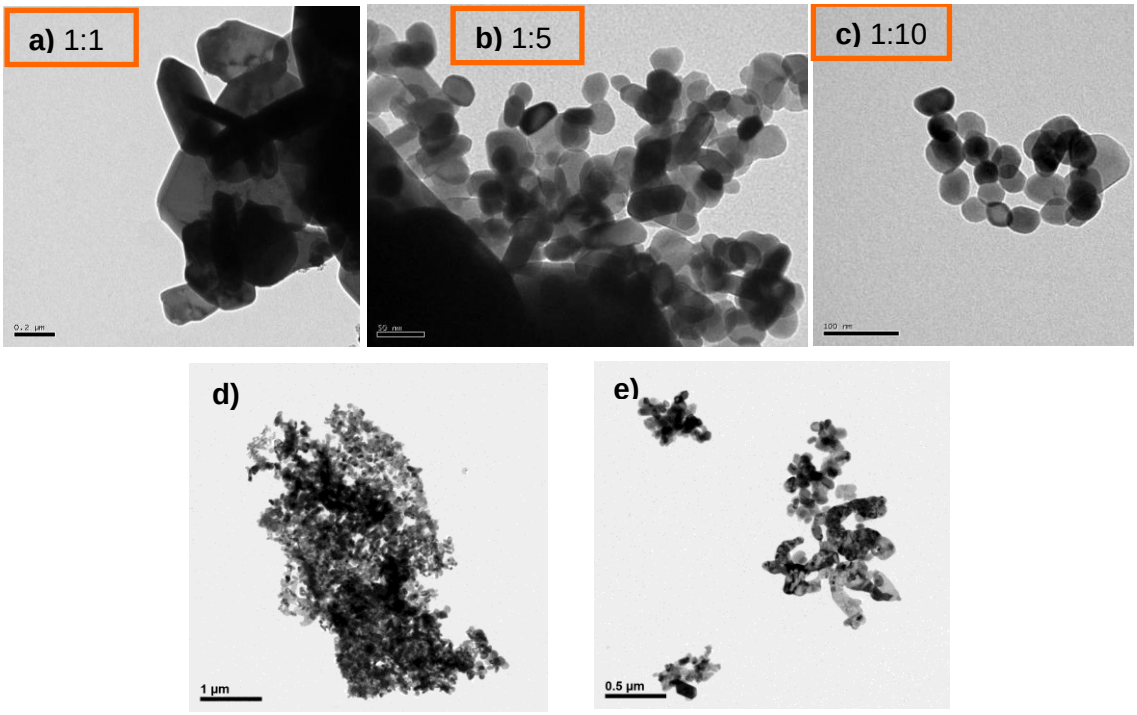

Figure 2.TEM a), b), c) HRTEM d), e) and EDS g) of Cr_2O_3.

On the other hand, the TEM image shows a no relationship of the size with the molar ratios for the Mo precursors. For the pyrolytic product from the precursors 1:1 Chitosan●$MoCl_3$, somewhat big bars nanostructures were observed see figure 3. The SAED image, figure 3 d, exhibits the presence of some planes characteristic of MoO_3 as (1 3 0), (1 4 0), (1 5 0), (0 0 2), (2 1 1), y (1 8 0). In figure 3 e, the EDS of the sample exhibits the presence of the O and Mo elements expected for MoO_3. HRTEM image (figure 3d) confirmed the structure of WO_3. The inset shows a SAE of the area with the zone axis [010].

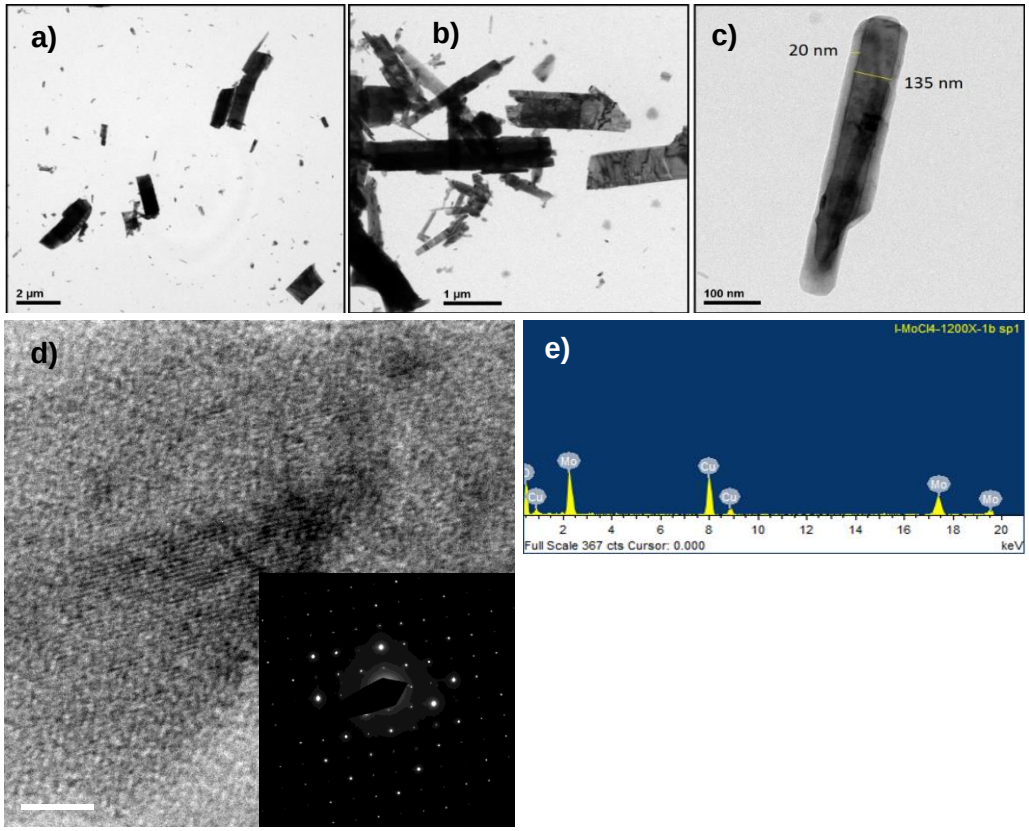

Figure 3. TEM a), b), c), SAE and HRTEM d) and EDS e) of MoO_3 from the 1:1 Chitosan●$MoCl_3$ precursor.

For WO_3 particles, as shown in figure 4, big agglomerates were observed. HRTEM images (figure 3d) confirmed the structure of WO_3, as the interplanar distance of 0.37 nm (020) was measured in both images. EDS analysis see figure 4e, as expected confirms the presence of W and O elements.

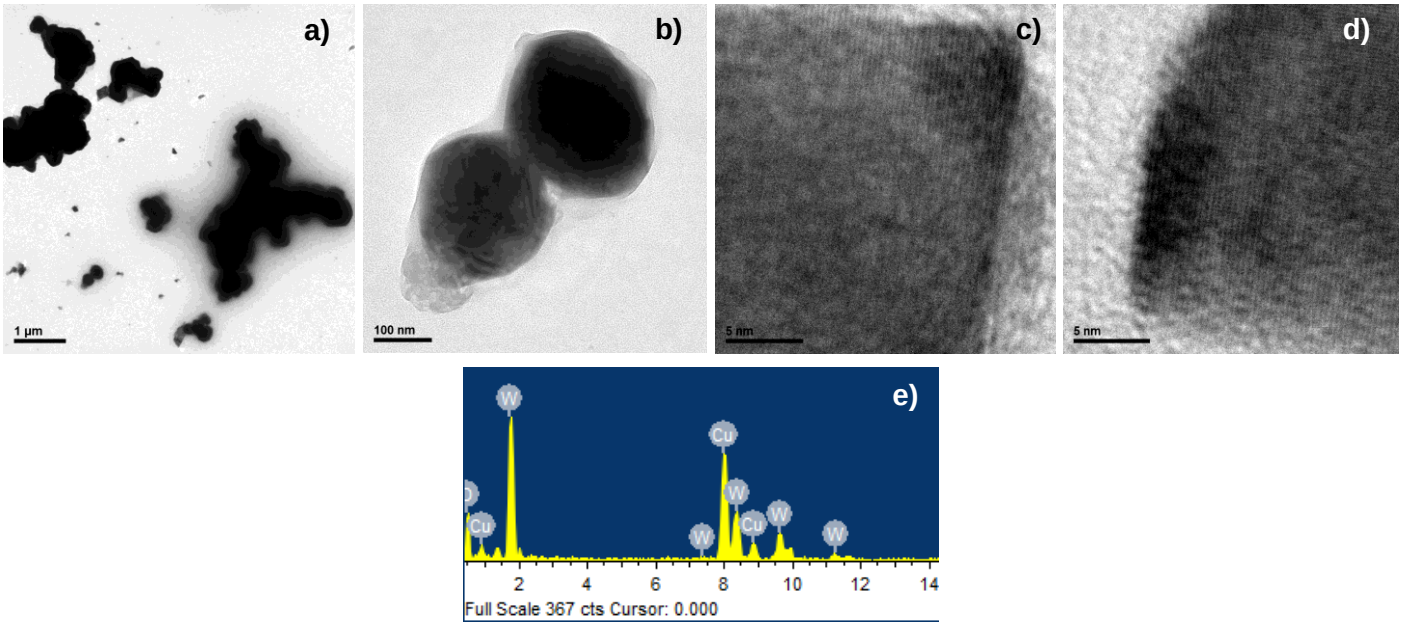

Figure 4. TEM a) and b) and HRTEM image c) d) and EDS e) of WO_3 from PS-co-4-PVP●WCl_4 precursors.

Inclusion of Cr_2O_3 and WO_3 inside silica

Owing the most applications of nanostructured Cr_2O_3 and WO_3 involves the use of these metal oxides inside SiO_2 (for instance catalysis) we attempted the inclusion of Cr_2O_3 and WO_3 inside silica using the here described solution-solid state method. SiO_2 was generated by the sol-gel method and added over the solution were the precursor PS-co-4-PVP●MXn and Chitosan●MXn with M= Cr and W was forming [71]. Then the PS-co-4-PVP●MXn//SiO_2 and Chitosan●MXn//SiO_2 precursors were pyrolyzed forming the Cr_2O_3//SiO_2, $MoCl_3$//SiO_3 and WO_3//SiO_2 composites. The X-ray analysis of the respective materials are shows in supplementary materials see figure S4.

The composite Cr_2O_3//SiO_2 and WO_3//SiO_2 obtained both, from the Chitosan●$CrCl_3$//SiO_2 as well as from PS-co-4-PVP●WCl_4//SiO_2 precursors exhibit the typical diffraction peaks of Cr_2O_3 or WO_3 discussed already, as well as a broad peak between 2θ = 15-20 ° for the Cr_2O_3//SiO_2 composite and a broad peak between 2θ = 5-20 ° for the WO_3//SiO_2 typical of amorphous silica [71-74].

The distribution of the metal oxides Cr_2O_3 and WO_3 was investigated using the SEM-EDS mapping technique. For both composites Cr_2O_3//SiO_2 and WO_3//SiO_2, a uniform distribution of the Cr_2O_3 and WO_3 of the nanoparticles inside SiO_2 was observed as is shows in figure 5 a) and 5b) and 6a) and b).

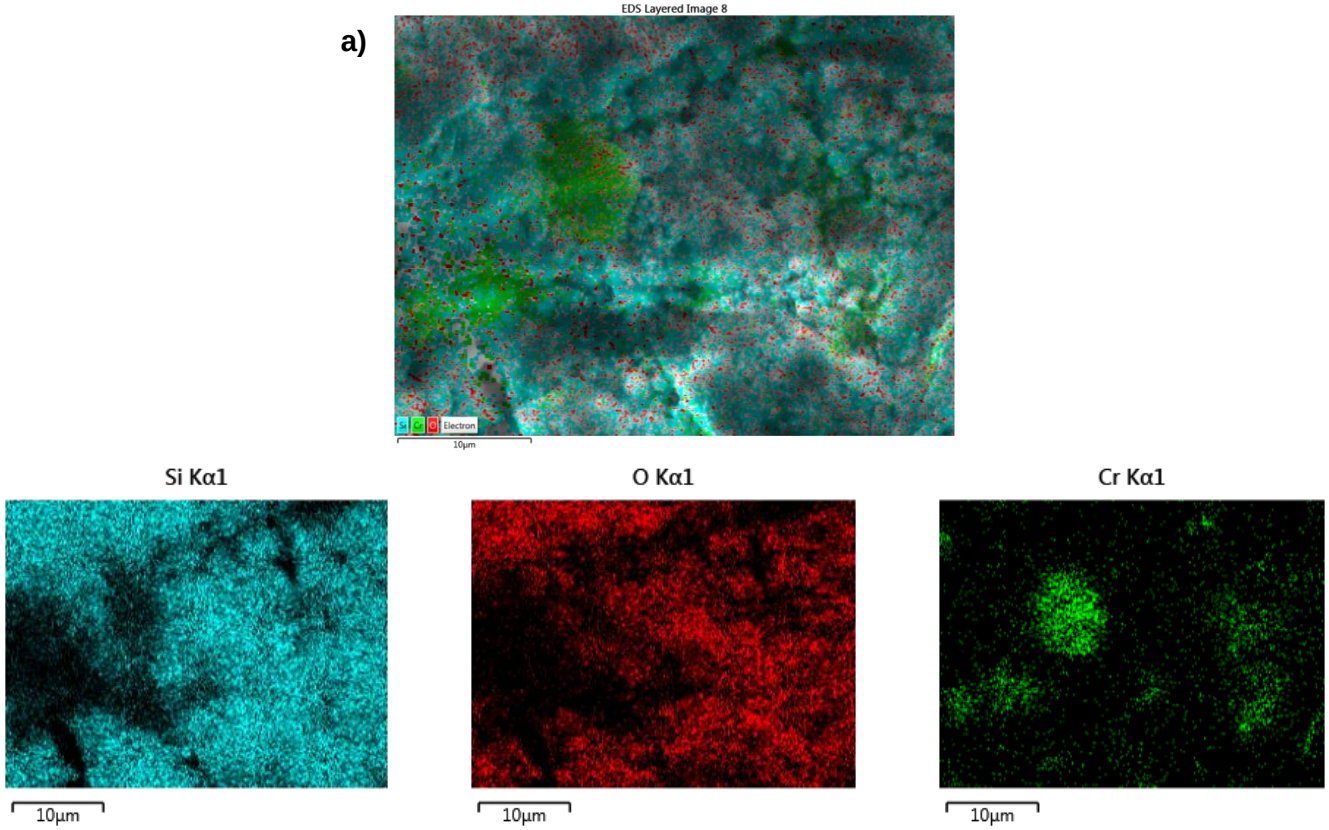

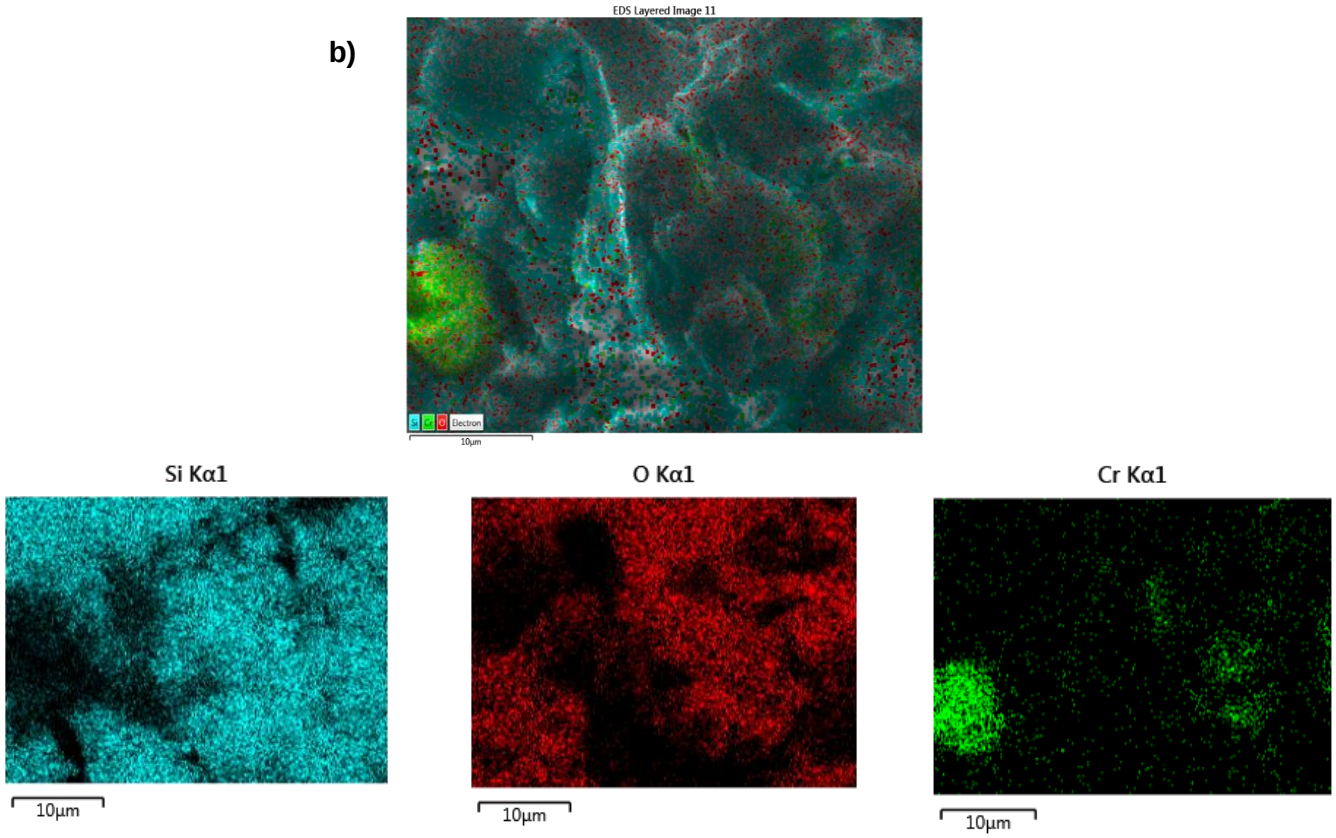

Figure 5. EDX-elemental mapping of a) Cr_2O_3 nanoparticles inside silica from PS-co-4-PVP●$(CrCl_3)_X$//SiO_2 precursor and of b) Cr_2O_3 nanoparticles inside silica from precursor Chitosan●($CrCl_3)_X$ //SiO_2.

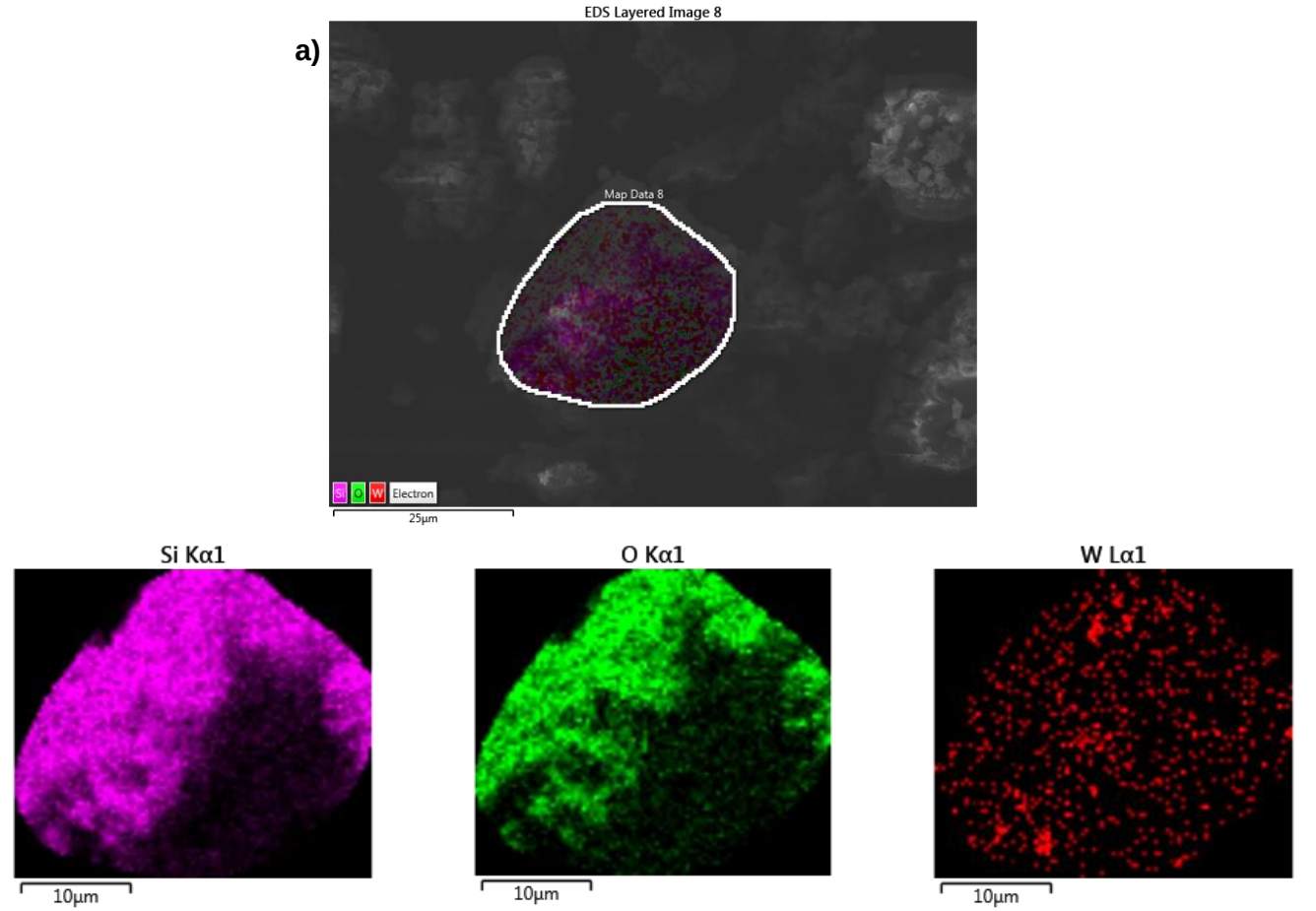

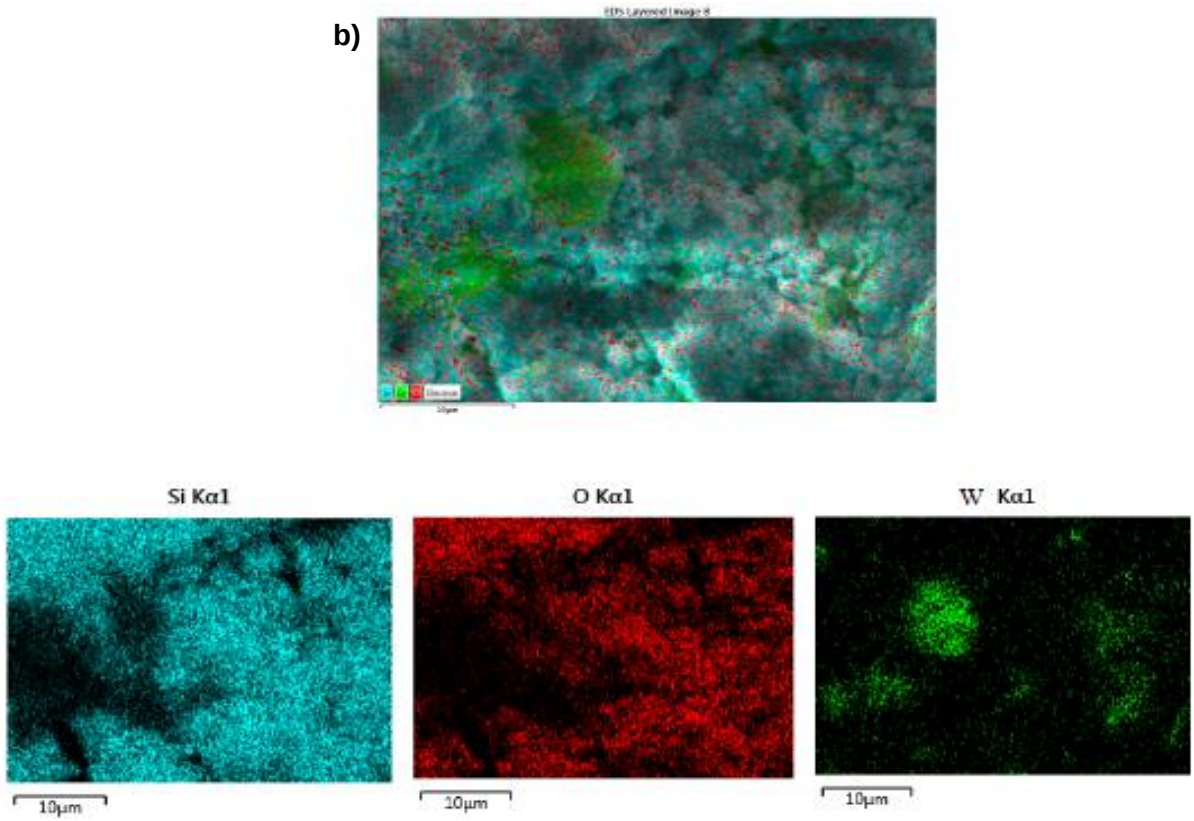

Figure 6. EDX-elemental mapping of a) WO_3 nanoparticles inside silica from PS-co-4-PVP●$WCl_4)_X$ //SiO_2 precursor and of b) WO_3 nanoparticles inside silica from precursor (Chitosan●$(WCl_4)_X$ //SiO_2.

Formation Mechanism of the Cr_2O_3, MoO_3 and WO_3 nanoparticles.

In order to give some insight about the formation mechanism of the nanostructured Cr_2O_3, MoO_3 and WO_3, we believe that materials from both precursors can be proposed using the mechanism of formation of nanostructured metallic materials from the oligomer precursor {$NP(OC_8H_{12})_2(OC_6H_4PPh_2$-$Mn(CO)_2(\eta^5$-$C_5H_4Me)_2\}_n$ [9,75]. A schematic representation of this process is provided in figure 7. Briefly, the first step on heating involves the formation of a 3D network to produce a thermally stable matrix. This step is crucial because it offsets the sublimation. The first heating step could involve a cross linking of the chitosan or PSP-4-PVP polymer giving a 3D matrix containing the Cr_2O_3, MoO_3 and WO_3, compounds linked to the polymeric chain.

The following steps could involve the starting of the organic carbonization, producing holes where the nanoparticles begin to nucleate. As it was confirmed in earlier studies [9,75], the Cr_2O_3, MoO_3 and WO_3 could grow over layered graphitic carbon host which is lost near to the final annealing temperature ie. 800 °C.

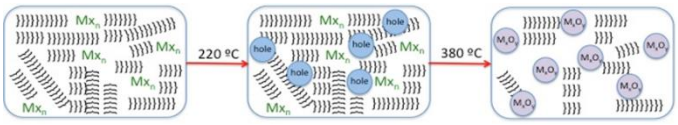

Figure. 7. Schematic representation of the proposed mechanism of formation of the metal oxide nanoparticles M_xO_y = Cr_2O_3, MoO_3 and WO_3. MX_n represent the general formula of the metallic salt coordinated to the Chitosan or PSP-4-PVP polymer and }}}}}}} represent the respective polymeric. The temperature are referential general values.

CONCLUSIONS

The series of nanostructured Cr_2O_3, MoO_3 and WO_3 oxides can be in pure phase obtained from the solid-state method using as precursors the macromolecular complexes PS-co-4-PVP●MCln and Chitosan●MCln with M= Cr, Mo and W by thermal treatment. Similarly, the composites Cr_2O_3//SiO_2, $MoCl_3$//SiO_2 and WO_3//SiO_2 were prepared from thermal treatment of the PS-co-4-PVP●MCln//SiO_2 and Chitosan●MCln//SiO_2. In these materials, the Cr_2O_3, MoO_3 and WO_3 oxides exhibited, in general, a uniform dispersion inside the silica matrix, which suggests a possible catalytic activity of these materials. The investigation of the optical properties of Cr_2O_3, MoO_3 and WO_3 and the effect on the inclusion inside the SiO_2 are in course.

ACKNOWLEDGEMENTS

The authors acknowledge Fondecyt Projects 1160241, for financial support. Also thanks to Professor Antonio Laguna of the Institute of Nanoscience and Materials of Aragón (INMA), CSIC-University of Zaragoza, 50009 Zaragoza, Spain for the HRTEM measurements and analysis.

COMPLIANCE WITH ETHICAL STANDARDS

Competing interests, the authors declare that they have no competing interests.

REFERENCES

1. D.Worle, A.D. Pomaglio (2003). "Metal Complexes and Metals in Macromolecules" Wiley-VCH
2. C. Díaz and M.L. Valenzuela (2006) in Polymer Research Developments, "Coordination of Organometallic Fragments to Polyphospahzenes Containing Side Groups with Donor Atoms". R.K. Bregg Ed. Nova Science Publishers, New York Pp 1-22.
3. G.A. Carriedo, F.J. Garcia-Alonso, J.L. García Alvarez, C. Diaz, N. Yutronic (2002) *Polyhedron* **21**, 2587-2592.
4. G.A. Carriedo, F.J. Garcia-Alonso, P. A. González, C. Diaz, N. Yutronic (2002) *Polyhedron* **21**, 2579-2586.
5. C. Diaz, P. Castillo, G.A. Carriedo, P. Gomez-Elipe, F.J. Garcia-Alonso (2002). *Macromolec. Phys. and Chem*. **203**, 1918-1925.
6. C. Díaz, M.L. Valenzuela (2006). *Macromolecules* **39**, 103-111.
7. C. Díaz, M.L. Valenzuela (2006). *Journal Inorganic and Organometallic Polymer and Materials* **16**, 419-435.
8. C. Díaz, M.L. Valenzuela, L. Zuñiga, C. O'Dwyer (2009). *Journal Inorganic and Organometallic Polymer and Materials*. **19**, 507- 520.
9. C Díaz, M.L. Valenzuela, V. Lavayen, C. O'Dwyer (2012). *Inorganic Chem*. **51**, 6228-6236.

10. C. Zhang, J. Chen, Y. Zeng, X. Rui, J. Zhu, W. Zhang, Ch.Xu, T.M. Lim, H.H.Hng, Q. Yan (2012). *Nanoscale* **4**, 3718-3724.
11. P. Poizot, L.S. Grugeon, L. Dupont, J-M Tarascon (2000). *Nature* **407**, 496-499.
12. Y. Li, A. Somorjai (2010). *Nano.Lett*. **10**, 289-2295.
13. F. Bozon-Verduraz, F. Fievet, J.Y. Piquemal, R. Brayner, K. Kabouss, Y. Soumare, G. Viau, G. Shaffev (2009). *Braz. J. Phys*. 134-140.
14. A. Tricoli, M. Righettoni, A. Teleki (2010) *Angew. Chem. Int. Ed*. **49**, 7632-7659.
15. P. Kamat (2012). *J. Phy.Chem. C* **116**, 11849-11851.
16. H. Huang, B. Liang, X, Wang, D. Chen, G. Shen (2012). *Journal of Material Chemistry* **22**, 13428- 13445.
17. J.S. Hu, L.S. Zhong, W.G. Song, L.J. Wan (2008). *Adv. Mater*. **20**, 2977-2982.
18. Ch. Yan, D. Xue (2006). *J. Phys.Chem. B* **110**, 1581-1586.
19. N. Pinna, M. Niederberger (2008). *Angew. Chem. Int.Ed*. **47**, 5292-5304.
20. M. Fernandez-Garcia, A. Martinez-Arias, J.C. Hanson, J.A. Rodriguez (2004). *Chem.Rev*. **104**, 4063-4104.
21. M.L. Khan, A. Glaria, C. Pages, M. Monge, L.S. Macary, A. Maisonnat, B. Chaudret (2009). *J. Mat. Chem.* **19**, 4044-4060.
22. J.P. Jolivet, S. Cassignon, C. Chanea, D. Chiche, D. Durupthy, D. Portehault, (2010). *C.R Chimie* **13**, 40-51.
23. C. Díaz, M.L. Valenzuela (2010) in *Encyclopedia of Nanoscience and Nanotechnology*, "Metallic Nanostructures Using Oligo and Polyphosphazenes as Template or Stabilizer in Solid State" H.S Nalwa Ed., American Scientific Publishers **16**, 239-256.
24. A. Orlov, A. Roy, M. Lehmann, M. Driess and S. Polarz (2007). *J. Am. Chem. Soc*. **129**, 371-375.
25. G. Walkers, I.P. Parkin (2009). *J. Mater. Chem*. **19**, 574-590.
26. M. Meilikhov, K. Yusenko, D. Esken, S.A. Turner, G. Van Tendolo, R.A. Fischer (2010). *Eur. J. Inorg. Chem*. 3701-3714.
27. B. Teo, X. Sun (2007). *Chem. Rev*. **107**, 1454-1532.
28. G.B. Khomutov, V.V. Kislov, M.N. Antipirina, R.V. Gainutdinov, S.P. Gubin, A.Y Obydenov, S.A. Pavlov, A.A. Rakhnyanskaya, A.N. Sergeev-Cherenkov, E.S. Soldatov, D.B. Suyatin, A.L. Toltikhina, A. S. Trifonov, T.V. Yurova (2003). *Microelectronic Engineering* **69**, 373-383.
29. K. Lee, W.S.Seo, Park (2003). *J. Am. Chem. Soc*. **125**, 3408-3409.
30. S. U. Son, Y.Jang, K.Y. Yoon, Ch. An, Y. Hwang, J-G.Park, Han-Jin Noh, Jae-Young Kim, Jae-Hoon Park, T. Hyeon (2005). *Chem Comm*. 86-88.
31. D. Parvis, E.M.Kazemeini, A.M. Rashidi, Kh. Josan (2010). *J. Nanopart. Res*. **12**, 1509-1521.
32. S.M. El-Sheikh, R.M. Mohamed, A.O. Fouad (2009). *J. Alloys Comp.* **482**, 302-307.
33. M. Aghaie-Khafri, M.H. Kakaei (2012). *Powder Technology* **222**, 152-160.
34. D. Chen, M. Liu, L. Yin, T. Li, Z. Yang, X. Li, B. Fan, H. Wang, R. Zhang, Z. Li, H. Xu, H. Lu, D. Yang, J. Sun, L. Gao (2011). *J. Mater. Chem*. **21**, 9332-9342.
35. H.M. Martínez, J. Torres, L.D. López-Carreño, M.E. Rodríguez-García (2013). *Materials Characterization* **75**, 184 – 193.
36. X. Huang, H. Liu, X. Zhang, H. Jiang (2015). *ACS Appl. Mater. Interfaces* **7**, 27845−27852
37. R. Huirache-Acuñaa, F. Paraguay-Delgadoc, M.A. Albiterd, J. Lara-Romerod, R. Martínez-Sánchezc (2009). *Materials Characterization* **60**, 932 – 937
38. C. Díaz, P. Castillo, M. L. Valenzuela (2005). *Journal of Cluster Science* **16**, 515-522.
39. K. Desai, K. Kit, J. Jiajie, S. Zivanovic (2008). Biomacromolecules **9**, 1000-1006.
40. Q. Li, E.T. Dunn, E.W. Grandmaison, M.F.A. Goosen (1992). *J. Bioactive and Compatible Polymers* **7**, 370-397.
41. I. Aranaz, M. Mengibar, R. Harris, I. Paños, B.Miralles, N.Acosta, G. Galed and A. Heras (2009). *Current Chemical Biology* **3**, 203-230.
42. R.B. Hernandez, O. Reyes, A.L. R. Merce (2007). *J. Braz. Chem.Soc*. **18**, 1388-1396.
43. I.S. Lima, C. Airoldi (2004). *Thermochim. Acta* **421**, 133-139.
44. E. Taboada, G. Cabrera, G. Cardenas (2003). *J. Chil. Chem. Soc*. **48**,
45. K. Ogawa, K. Oka (1993). *Chem. Mater*. **5**, 726-728.
46. S. Schlick (1986). *Macromolecules* **19**, 192-195.
47. J. Brugnerotto, J. Lizardi, F.M. Goycoolea, W.Arguelles-Monal, J. Desbrieres, M. Rinaudo (2001). *Polymer* **42**, 3569-3580.
48. H. Huang, X. Yang (2004). *Carbohydrate Research* **339**, 2627-2631.
49. Y. Ding, X.H. Xia and C. Zhang (2006). *Nanotechnology* **17**, 4156-4162.
50. M. Adlim, M.A. Bakar, K. Kong Live, J. Ismail (2004). *J. Mol. Cat.* **212**, 141-149.
51. K. Okitsu, Y. Mizukoshi, T. A. Yamamoto, Y. Maeda and Y. Nagata (2007). *Mater. Lett.* **61**, 3429-3431.
52. K.H. Yang, Y.Ch. Liu, T.Ch. Hsu, H.I. Tsai (2010). *Mater.Research Bulletin* **45**, 63-68.
53. I. Zhitomirsky, A. Hashambhoy (2007). *J. Mater. Proc. Tech*. **191**, 68-72.
54. H. Huang, Q. Yuan, X. Yang (2004). *Colloids and Surfaces B: Biointerfaces* **39**, 31-37.
55. Y.Ch. Chang, D.H. Chen (2005). *Journal of Colloid and Interfaces Science* **283**, 446-451.
56. L. Ding, Ch. Hao, Y. Xue, H. Ju (2007). *Biomacromolecules* **8**, 1341-1346.
57. Y. Du, X.L. Luo, J.J. Xu, H. Y. Chen (2007). *Bioelectrochemistry* **70**, 342-347.
58. X.L. Luo, J.J. Xu, Q. Zhang, G.J. Yang and H.Y.Chen (2005). *Biosensors and Bioelectronics* **21**, 190-196.
59. E. Guibal (2005). *Prog. Polym.* Sci. **30**, 71-109.
60. B. Geng, Z.Jin, T. Li and X. Qi (2009). *Sci. Total Environ*. **407**, 4994-5000.
61. P. Guo, W. Wenyan, G. Liang, P. Yao (2008). *J. Colloid Interface Sci.* **323**, 229-234.
62. L. A. Belfiore, M. P. Curdie and E. Ueda (1993). *Macromolecules* **26**, 6908-6919.
63. A. Haynes, P. M. Maitlis, R. Quyoum, C. Pulling, H. Adams, S. E. Spey, R.W. Strange (2002). *J. Chem. Soc. Dalton Trans.* 2565-2572.
64. C. V. Franco, M. M. da SilvaPaula, G. Goulart, L. F. De Lima, L. K. Noda, N. S. Gonçalves (2006). *Mater. Lett.* **60**, 2549-2553.
65. F. Wen, W. Zhang, G. Wei, Y. Wang, J. Zhang, M. Zhang, L. Shi (2008). *Chem. Mater.* **20**, 2144-2150.
66. S. Klingelfer, W. Heitz, A. Greiner, S. Oestreich, S. Forster, M. Antoinietti (1997). *J. Am. Chem. Soc.* **119**, 10116-10120.
67. P. Zheng, X. Jiang, X. Zhang, L. Shi (2006). *Langmuir* **22**, 9393-2396.
68. C. Diaz, M.L. Valenzuela, G. Carriedo N. Yutronic (2014). *J. Chil. Chem. Soc.* **59**, 2437-2441.
69. C. Díaz, V. Lavayen, C. O'D wyer (2010). *J. Solid St. Chem* **183**, 1595-1603.
70. C. Díaz, M.L. Valenzuela, N. V. Lavayen, K. Mendoza, O. Peña, C. O'Dwyer (2011). *Inorg. Chim. Acta*. **377**, 5-13.
71. C. Díaz, M.L. Valenzuela, M. Segovia, R. De la Campa, A. Presa-Soto (2018). *J. Clust. Sci.* **29**, 251–266.
72. G. Yang, H. Yang, X. Zhang, K. lqbal, F. Feng, J. Ma, J. Qin, F. Yuan, Y. Cai, J. Ma (2020). *Journal of Hazardous Materials* **397**, 122654.
73. D. Li, G. Wu, G. Gao, J. Shen, F. Huang (2011). *ACS Appl. Mater. Interfaces* **3**, 4573–4579.
74. M.V. Borysenko, V.M. Bogatyrov, E.N. Poddenezhny, A. A. Boiko, A.A. Chuiko (2004). *Journal of Sol-Gel Science and Technology* **32**, 327–331.
75. C. Díaz, M.L. Valenzuela, M.A. Laguna-Bercero, A. Orera, D. Bobadilla, S. Abarca, O. Peña (2017). *RSC Advances* **7**, 27729-27736